Drought and mistletoe reduce growth and water-use efficiency of Scots pine

Gabriel Sangüesa-Barreda[1], Juan Carlos Linares[2] and J. Julio Camarero[3,4]*

[1]Instituto Pirenaico de Ecología (CSIC). Avda. Montañana 1005, Apdo. 202, 50192 Zaragoza, Spain.

[2]Departamento de Sistemas Físicos, Químicos y Naturales, Universidad Pablo de Olavide. Ctra. Utrera km. 1, 41002 Sevilla, Spain.

[3]ARAID, Instituto Pirenaico de Ecología (CSIC). Avda. Montañana 1005, Apdo. 202, 50192 Zaragoza, Spain.

[4]Dept. d'Ecologia, Fac. Biologia, Universitat de Barcelona. Avda. Diagonal 645, 08028 Barcelona, Spain.

*Corresponding author:

Dr. J. Julio Camarero

E-mail: jjcamarero@ipe.csic.es

Tel. 0034-976-716031, Fax: 0034-976-716019

ABSTRACT

To what extent do mistletoes contribute to growth decline in drought-prone forests? Can the rising atmospheric CO_2 concentrations offset the negative impacts of drought and mistletoe infestation on tree growth? Long-term data on growth and intrinsic water use efficiency (iWUE) may allow answering both questions. We used dendrochronology to assess long-term changes in radial growth and iWUE in Scots pine (*Pinus sylvestris*) trees severely infested by mistletoe (*Viscum album*) as compared to non-infested trees. The relationships among tree variables and mistletoe infestation were quantified using structural equation models. Linear mixed-effects models of basal area increment as a function of climate were fitted to severely infested and non-infested trees. Infested trees showed higher stem and crown diameters because they grew faster than non-infested trees in the past. Mistletoe infestation enhanced defoliation and reduced radial growth for more than ten years prior to sampling, while iWUE was significantly lower on severely infested trees only for the last five years. Severely infested trees had higher growth responsiveness to drought stress than non-infested trees. Although infested and non-infested trees displayed similar rising iWUE temporal trends, the combined effect of drought stress and mistletoe infestation caused a reduction in growth and reversed the CO_2-induced increase of iWUE in infested trees. We conclude that rising atmospheric CO_2 concentrations can not compensate for the impacts of drought and mistletoe on tree growth and iWUE.

Key words: basal area increment; dendrochronology; intrinsic water-use efficiency; *Pinus sylvestris*; *Viscum album*.

1. Introduction

Do mistletoes contribute to drought-induced forest decline (*sensu* Allen et al., 2010) by altering carbon and water use in trees? Mistletoes are usually regarded as biotic factors contributing to forest decline in areas with moderate to severe water deficit (Tsopelas et al., 2004; Dobbertin et al., 2005). However, mistletoes may also be predisposing factors (*sensu* Manion, 1991) by weakening host trees or inducing growth loss and enhanced defoliation in severely infested trees (Dobbertin and Rigling, 2006; Galiano et al., 2010). In this sense, Rigling et al. (2010) suggested that mistletoe infestation makes trees more vulnerable to drought stress when growing in a xeric site.

Global change components may have contrasting effects on mistletoe-tree interactions driving different trajectories of tree growth and vigour, and leading to divergent carbon balances at the stand level. First, rising air temperatures increase warming-induced drought stress which is sometimes exacerbated by mistletoe infestation on host trees due to the high transpiration rates of the hemiparasite (Dobbertin and Rigling, 2006). In addition, a warmer climate might also promote the expansion of some mistletoe species whose distribution area is mainly controlled by low temperatures (Dobberttin et al., 2005). Second, rising CO_2 concentrations in the atmosphere might benefit host trees through a fertilization effect increasing their photosynthetic rates and leading to higher growth rates in the tree and plausibly in the mistletoe (Bickford et al., 2005). If the elevated CO_2 leads to enhanced carbon uptake and growth stimulation through increasing intrinsic water-use efficiency (iWUE) such responses could alleviate the negative effects caused on host trees by the carbon and water removed from them by the mistletoe. However, this argument relies on the assumption that other factors (mesophyll conductance, evaporative demand) play a secondary role on iWUE changes which is not always the case (Seibt et al., 2008; Roden and Farquhar, 2012).

However, increasing iWUE with rising atmospheric CO_2 concentration is not leading to improved tree growth everywhere (Peñuelas et al., 2010) suggesting that tree growth does not seem to be limited by carbon supply (Körner, 2003). Indeed, tree growth has not been stimulated as expected in response to the CO_2 increase and it has remained stable or even declining in some areas, suggesting that other local factors override the expected CO_2 fertilization effect (Martinez-Vilalta et al., 2008; Linares and Camarero, 2011). Hence, the extent that rising CO_2 may enhance tree growth and whether drought stress and mistletoe infestation could explain deviations from the projected CO_2-induced growth enhancement are still poorly understood in trees heavily affected by mistletoe living in drought-prone areas.

Several studies using $^{13}C/^{12}C$ isotopic ratios in annual tree rings show that trees respond to increasing atmospheric CO_2 concentrations in diverse ways, suggesting an interaction with other local environmental factors (Ferrio et al,. 2003; Saurer et al., 2004). Climate warming-related drought and long-term acclimation to elevated CO_2 concentrations have been proposed as potential factors constraining the expected fertilization effect (Linares and Camarero, 2011). However, to the best of our knowledge no study has yet tackled the role of mistletoe infestation on driving changes in iWUE trends in response to rising CO_2 concentrations.

Mistletoes are aerial hemiparasitic plants which take water and carbohydrates from host trees (Glatzel and Geis, 2009). Mistletoes are also keystone species for maintaining biodiversity since their fruits feed several bird species during the winter (Mathiasen et al., 2008). Scots pine (*Pinus sylvestris* L.), the conifer with the widest geographical distribution area in the world, is the host of the European pine mistletoe (*Viscum album* ssp. a*ustriacum* L.; Zuber, 2004). Iberian Scots pine populations make up the southernmost distribution limit of the species and thus these stands are expected to be very vulnerable to drought-induced decline, particularly in xeric sites (Martinez-Vilalta and Piñol, 2002).

Here, we use dendrochronology to retrospectively assess long-term changes in growth and water-use efficiency in four Scots pine forests heavily affected by mistletoe and located near the southern margin of the species' distribution area in eastern Spain. Our specific objectives were: (*i*) to determine the relationships between different variables measured in host tress (diameter measured at 1.3 m, total height, crown height and diameter, crown cover, basal area increment, and sapwood area) and mistletoe infestation and to determine how this in turn affects tree defoliation and basal area increment, and (*ii*) to quantify how the combined stressing effects of drought and mistletoe infestation drive changes in basal area increment and iWUE.

2. Materials and methods

2.1. Study area and field sampling

The study area includes four Scots Pine (*Pinus sylvestris* L.) forests located in the Iberian System (Alcalá de la Selva, Teruel province, Aragón), eastern Spain, near the southern distribution limit of the species (Table 1; Supplementary Material, Fig. S1). We selected four sites dominated by Scots pine and showing different topographical (altitude, slope) and structural (basal area, stem density) characteristics, and containing at least ten dominant trees heavily infested by mistletoe (Tables 1 and 2). The vegetation is dominated by *P. sylvestris*,

junipers (*Juniperus sabina* L., *J. communis* L.) and shrubby species (*Berberis vulgaris* L., *Genista scorpius* L.). The soils are basic and calcareous. The climate in the study area is Mediterranean with continental influence according to local meteorological of the station "Alcalá de la Selva-Solano de la Vega" located at ca. 3 km from the study sites. The mean annual temperature is 9.4 ºC and the annual precipitation is 670 mm (Supplementary Material, Fig. S2). During the period 1987-2008 no seasonal climatic variable showed significant long-term trends while for the late 20th century temperature significantly rose only in fall (Supplementary Material, Fig. S2).

The size (diameter at 1.3 m or at breast height –dbh–, total height, crown height and diameter −the later was based on the average of two horizontal crown diameters measured along N-S and E-W directions−) and the crown cover (in %) of all trees with dbh > 15 cm and located within a plot 30 m x 30 m were measured. To estimate crown defoliation (a proxy of crown transparency) we measured in the field crown cover (amount of crown stem, branches, twigs, shoots, buds, needles and reproductive structures that block light penetration through the crown), i.e. the opposite of crown defoliation. Crown cover was used as a proxy of tree vigor following Dobbertin (2005). Crown cover was measured in 5-percent classes following Schomaker et al. (2007). Since estimates of percent crown cover may vary among observers and places, we used as a reference a tree with the maximum amount of foliage at each site and this variable was always measured by the first author.

The mistletoe infestation degree (ID) was estimated using a modified 3-class rating system based on the original scale established by Hawksworth (1977). The tree crown was vertically divided in three similar sectors and each third was classified as 0 (absence of mistletoe) or 1 (presence of mistletoe) (see examples of severely infested trees in the Supplementary Material, Fig. S3). Then, the total mistletoe abundance or infestation degree of each tree was obtained summing the rates of each crown third. Mistletoe abundance ranged from 0 to 3 and all analyses were done based on three classes of abundance or infestation degree (ID): trees without mistletoes (ID = 0, class ID1), moderately infested trees with mistletoe present in one or two thirds of the crown (ID = 1-2, class ID2) and severely infested trees with mistletoe present throughout the crown (ID = 3, class ID3). Tree variables were compared among trees of different infestation degrees in each of the study sites using ANOVAs. Variables expressed as percentages (e.g., crown cover) were previously arcsine-square-root transformed.

124 *2.2. Climate data*

125 To obtain a robust regional climatic series, local data from four meteorological stations
126 located from 5 up to 30 km away from the study site were combined into a regional mean for
127 the period 1954-2008 (Supplementary Material, Table S1). To estimate the missing data for
128 each station, and to combine them, we used the MET program from the Dendrochronology
129 Program Library (Holmes, 1994). For each station, monthly variables (mean temperature,
130 total precipitation) were transformed into normalized standard deviations to give each station
131 the same weight in calculating the average monthly values for each year. The difference in the
132 mean elevations of study sites and meteorological stations (on average 300 m) may imply
133 slightly lower temperature values (on average −1.0 ºC) and higher annual precipitation
134 amounts (ca. +55 mm) than in nearby stations.

135 We calculated a regional cumulative water budget using a modified Thornthwaite
136 water-budget procedure based on monthly climatic data (mean temperature and total
137 precipitation; see Willmott et al., 1985) and assuming a soil water holding capacity of 125
138 mm based on published data on soil types in the study area (Mapas Provinciales de Suelos,
139 1970). Soil water balance was modelled by estimating soil-water withdrawal, recharge, and
140 surplus. Positive and negative values correspond to wet and dry conditions, respectively. We
141 calculated the cumulative water deficit from January through June, when the study species
142 performs most of its growth in the study area (JJ Camarero, *pers. observ.*). Then, severe
143 drought events were defined as those years with the maximum cumulative water deficit values
144 (1986, 1994 and 2005). The mean cumulative water deficit (± SE) for the period 1954-2008
145 was −21.7 ± 21.2 mm, whereas values for the selected years were: −117.8 mm for 1986,
146 −165.4 mm for 1994 and −122.3 mm for 2005. Calculations were done by using the AET
147 software available at http://geography.uoregon.edu/envchange/pbl/software.html.

148

149 *2.3. Dendrochronological methods*

150 Sampling was performed at each site using standard dendrochronological methods (Fritts,
151 1976). Two cores were taken at 1.3 m using a Pressler increment borer from each tree located
152 within the 30 m x 30 m plot (see the total number of cored trees per site in Table 2). Sapwood
153 depth was measured in the field for each core and averaged for each tree to obtain an estimate
154 of sapwood area (%) which was calculated assuming a circular shape of the stem. The wood
155 samples were air-dried and polished with a series of successively finer sand-paper grits until
156 rings were clearly visible. The samples were visually cross-dated and a minimum of 50 cross-
157 dated trees (100 radii) were measured for each site. Tree rings were measured to the nearest

158 0.01 mm using a binocular scope and a LINTAB measuring device (Rinntech, Heidelberg,
159 Germany). Cross-dating of the tree rings was checked using the program COFECHA
160 (Holmes, 1983). Tree age at 1.3 m was estimated by counting rings in the oldest core of living
161 trees and by fitting a geometric pith locator to the innermost rings to estimate the distance
162 missing up to the theoretical pith. The estimated distance to the theoretical pith was also used
163 to correct the calculation of basal area increment which was calculated assuming a circular
164 shape of stems. The trend due to the geometrical constraint of adding a volume of wood to a
165 stem of increasing radius was corrected by converting tree ring widths into basal area
166 increments, which is a more biologically meaningful descriptor of growth trends than ring
167 widths (Biondi and Qaedan, 2008). Basal area increment, hereafter abbreviated as BAI, was
168 calculated from tree-ring widths as the difference between consecutive cross-sectional basal
169 areas (BA) estimated for years t+1 and t as:

170 $$BAI_{t+1} = BA_{t+1} - BA_t = \pi ((CL_t + TRW_{t+1})^2 - (CL_t)^2) \quad (1)$$

171 where CL is the core length measured for dated tree-rings formed in years t+1 and t and TRW
172 is the tree-ring width.
173
174 *2.4. Structural equation models*
175 Structural Equation Models (SEM; Grace, 2006) were used to statistically evaluate postulated
176 relationships between tree variables (dbh, crown cover, sapwood area), basal area increment
177 (mean value for the common period 1970-2008) and mistletoe infestation degree (see
178 Supplementary Material, Appendix 1). First, we specified several theoretical models based on
179 *a priori* assumed relationships among variables considering the available literature (Zuber,
180 2004; Dobbertin and Rigling, 2006; Rigling et al., 2010; Galiano et al., 2010, 2011). Second,
181 we tested if the variance-covariance matrix obtained from observational data significantly
182 differed from the matrix imposed by the hypothetical models. To perform SEM analyses we
183 selected a subset of all cored trees (n = 158 trees) in which all the aforementioned variables
184 have been measured and located at more than 5 m from the closest plot margin in order to
185 avoid edge effects (Table 2). To estimate SEMs we used the maximum likelihood method.
186 The use of several indices to evaluate the model fitness provides a robust assessment of the
187 fitted SEM (Jöreskog 1993). Hence, we evaluated the fiited models using the chi-square (χ^2)
188 test and its related probability level (P), as well as complementary goodness-of-fit indices
189 (AGFI, Adjusted Goodness-of-Fit Index; RMSEA, Root Mean Square Error of
190 Approximation; AIC, the Akaike Information Criterion). Values close to zero for the χ^2 and
191 RMSEA statistics and values close to one of the AGFI index would indicate that the evaluated

models are consistent with the theoretical ones. Lower AIC values correspond to more parsimonious models. In relative terms, models with low AIC and high *P* values associated with χ^2 correspond to better fits than models with the reverse characteristics. Since mistletoe infestation is an ordinal variable we also performed a Bayesian estimation using a Markov Chain Monte Carlo algorithm because this is the method suggested when ordinal variables are modeled as ordered-categorical data (Arbuckle, 1995-2009). Nevertheless, maximum likelihood estimates are usually robust when ordinal variables contain few categories as is the case of mistletoe infestation (Lee, 2007).

2.5. Linear mixed-effects models of basal area increment

We tested the following linear mixed-effects model of BAI (standardized data for the period 1954-2008):

$$yi = Xi\beta + Zibi + \varepsilon i \qquad (2)$$

where *yi* represents BAI, and β is the vector of fixed effects (i.e. climate variables), *bi* is the vector of random effects (i.e. tree dbh, tree identity and tree age at coring height), *Xi* and *Zi* are, respectively, fixed and random effects regressor matrices, *εi* is the within group error vector. Linear mixed-effects models of BAI were built separately for non-infested (class ID1, trees without mistletoe) and infested trees (class ID2, moderately infested trees, and class ID3, severely infested trees) considering the four study sites (SA, SB, PA, PB) to test if infested and non-infested trees show contrasting growth responses to climate. BAI of the previous year was introduced into the model as an additional fixed effect to account for the first-order temporal autocorrelation of this variable, while tree dbh was introduced as a random factor into the model to account for potential tree-size effects, and tree age was also introduced to account for potential tree-age effects. Residuals of the models were checked for normality, homoscedasticity and autocorrelation. The effects of climate on BAI were tested and compared with a null model considering BAI of the previous year as a constant (see Biondi and Qaedan, 2008). The random effects and the covariance parameters were estimated using the restricted maximum likelihood method (Zuur et al., 2009). We used an information-theoretic approach for multi-model selection (see Burnham and Anderson, 2002), based on the AIC corrected for small sample sizes (AICc). The AIC combines the measure of goodness of fit with a penalty term based on the number of parameters (*k*) used in the model, i.e. it selects the most parsimonious models. We also calculated Δ*i* (difference in AICc with respect to the best model) and *Wi* (relative probability that the model *i* was the best model for the observed data). We considered models with substantial support to be those in which the

226 ΔAIC, i.e. the difference of AICc between models, was less than 2 (Zuur et al., 2009). We
227 fitted linear mixed-effects models using the *nlme* library of the R statistical suite version 2.14
228 (R Development Core Team 2013)
229
230 *2.6. Changes in intrinsic water-use efficiency*
231 To compare the changes in intrinsic water-use efficiency (iWUE) of co-occurring non-
232 infested and infested Scots pine trees we measured $^{13}C/^{12}C$ isotope ratios in wood from cross-
233 dated annual tree rings during the late 20th century. For this purpose we sampled ten
234 additional trees located near the plot located in site PA. We randomly selected trees of similar
235 size and sampled them taking two additional cores at 1.3 m from five trees without mistletoe
236 (ID1) and five trees severely infested by mistletoe (ID3). The sampled trees were dominant
237 and of similar size and age (mean ± SE values: dbh = 22.1 ± 0.6 cm, mean height = 8.9 ± 0.2
238 m, mean age = 50.0 ± 4.3 years). Cores were cross-dated, sapwood length was measured, and
239 tree-ring width and basal area increment were measured as explained before (see
240 *Dendrochronological methods*).
241 Wood segments containing five contiguous annual tree-rings were carefully separated
242 with a razor blade with the help of a binocular microscope. Samples were grouped in 5-year
243 segments starting in 1970 (1970-1974, 1975-1979, 1980-1984, 1985-1989, 1990-1994, 1995-
244 1999, 2000-2004) and ending with a 4-year segment (2005-2008). We analyzed five-ring
245 instead of one-ring wood segments in this study to account for a large enough number of tree
246 individuals while maintaining mid to low frequency temporal variability. Wood samples were
247 carefully homogenized and milled using an ultra centrifugation mill (Retsch ZM1, mesh size
248 of 0.5 mm). An aliquot of 0.5–0.7 mg of each wood sample was weighed on a balance
249 (Mettler Toledo AX205) and placed into a tin capsule for isotopic analyses. Cellulose was not
250 extracted as both whole wood and cellulose isotope time-series show similar long-term trends
251 related to atmospheric CO_2 concentration and climate (Saurer et al., 2004). Furthermore, a
252 carryover effect from year to year would be negligible because we analyzed 4- or 5-year
253 segments. The isotopic ratio $^{13}C/^{12}C$ ($\delta^{13}C$) was determined on an isotope ratio mass
254 spectrometer (Thermo Finnigan MAT 251) at the Stable Isotope Facility (University of
255 California, Davis, USA). The results were expressed as relative differences in $^{13}C/^{12}C$ ratio of
256 tree material with respect to the Vienna Pee-Dee Belemnite (V-PDB) standard. Two analytical
257 standards were included for analysis after every ten wood samples: cellulose ($\delta^{13}C$ =-24.72‰)
258 and phthalic acid ($\delta^{13}C$ = -30.63‰). The repeated analysis of these two internal standards

yielded a standard deviation lower than 0.1‰ and the accuracy of analyses was 0.07‰. The estimated precision of the measurements was ±0.1‰.

Isotopic discrimination between the carbon of atmospheric CO_2 and plant carbon (Δ; see Farquhar and Richards, 1984) was defined as:

$$\Delta = (\delta^{13}C_{atm} - \delta^{13}C_{plant}) / (1+\delta^{13}C_{plant}/1000) \quad (3),$$

where $\delta^{13}C_{atm}$ and $\delta^{13}C_{plant}$ are the isotope ratios of carbon ($^{13}C/^{12}C$) in atmospheric CO_2 and plant material (tree rings and needles) respectively, expressed in parts per thousand (‰) relative to the standard V-PDB; Δ is linearly related to the ratio of intercellular (c_i) to atmospheric (c_a) CO_2 mole fractions, by (see Farquhar et al., 1982):

$$\Delta = a + (b-a)\, c_i/c_a \quad (4),$$

where a is the fractionation during CO_2 diffusion through the stomata (4.4‰), and b is the fractionation associated with reactions by Rubisco and PEP carboxylase (27‰; Farquhar and Richards, 1984). The values for variables c_a and $\delta^{13}C_{atm}$ were obtained from published data (see Table 2 in McCarroll and Loader, 2004). Since all sampled trees were located at similar elevation, a correction for differences in ambient CO_2 partial pressure was not needed.

The c_i/c_a ratio reflects the balance between net assimilation (A) and stomatal conductance for CO_2 (g_c) according to Fick's law: $A = g_c(c_a - c_i)$. Stomatal conductances for CO_2 and water vapour (g_w) are related by a constant factor ($g_w = 1.6g_c$), and hence these last two variables allow linking the leaf-gas exchange of carbon and water. The linear relationship between c_i/c_a and Δ may be used to calculate the intrinsic water-use efficiency (iWUE), defined as the ratio of net assimilation to stomatal conductance to water vapour (A/g_w), which is calculated as follows:

$$\text{iWUE} = (c_a / 1.6)\, [(b-\Delta) / (b-a)] \quad (5)$$

The iWUE (μmol mol^{-1}) inferred from $\delta^{13}C$ has been widely related to long-term trends in the internal regulation of carbon uptake and water loss in plants (see McCarroll and Loader, 2004; Robertson et al., 2008) assuming that Δ relates linearly to c_i/c_a, despite the iWUE is not equivalent to actual water use efficiency, which is the ratio of assimilation (gained carbon) to transpiration (lost water) (see Seibt et al., 2008).

3. Results

3.1. Relationships between mistletoe infestation, tree variables and growth

On average, 20% of sampled trees were severely infested by mistletoe (Table 2). Severely infested trees contained a mean number of 820 mistletoe individuals per tree and the oldest living mistletoes reached a maximum age of 30 years (results not presented). In all studied

sites, severely infested trees had thicker diameter (dbh) and wider crown but lower crown cover than non-infested trees, whereas in three out of four sites infested trees had less BAI and sapwood area than non-infested trees (Table 3). No significant differences in age were observed among trees of contrasting infestation degree.

The variable most strongly and positively related to infestation degree was the tree diameter (Fig. 1). The mistletoe infestation degree drove BAI decline, both directly by reducing radial growth and indirectly by decreasing crown cover. The sapwood area was positively related to crown cover and BAI, while the tree diameter was also positively related to cover but negatively to BAI. Lastly, the two methods of SEM estimation (maximum likelihood *vs*. bayesian estimations) yielded similar results (Supplementary Material, Table S2).

3.2. Effects of drought and mistletoe on basal area increment

Currently infested trees showed in the past higher BAI values than non-infested trees. We found noticeable BAI decreases during severe droughts for both non-infested and infested trees (Fig. 2). Growth of infested trees has steadily declined since the 1994 severe drought in those sites where these trees showed the lowest BAI levels (e.g., sites SA and PA; Table 3).

On average, the previous-year BAI explained about 15% of total BAI variance (Table 4; see also all fitted linear-mixed effects models used to predict tree BAI in the Supplementary Material, Table S3). The selected linear-mixed effects models showed that the most significant climate driver of BAI was the negative effect of spring-to-summer temperatures (about 38 % of the explained variance), whereas BAI was also positively affected by previous autumn rainfall (3%) and spring-to-summer rainfall (4%). Previous autumn temperature was negatively related to BAI and this effect was more intense in trees infested by mistletoe (8 %) than in non-infested trees (3%; see Table 4). Previous December temperature showed a positive effect on BAI, being also slightly higher in infested (5%) than in non-infested trees (2%). On average, the total variance explained by climate was slightly higher for trees infested by mistletoe (56%) than in non-infested trees (50%). Finally, infested and non-infested trees showed similar patterns in their BAI residuals (see Supplementary Material, Fig. S4).

3.3. Effects of drought and mistletoe on iWUE

Non-infested and severely infested trees showed similar long-term trends in $\delta^{13}C$, Δ and iWUE until 2005 (Fig. 3). Severely infested trees usually had lower iWUE values than non-

infested trees. In the interval 2005-2008 severely infested trees had a significantly lower iWUE than non-infested trees (F = 5.64, P = 0.044). Such difference appeared because in severely infested trees the iWUE stabilized at 105 μmol mol^{-1}, i.e. they stopped rising their iWUE, whereas the non-infested trees decreased in discrimination and consequently their iWUE increased up to 114 μmol mol^{-1}.

4. Discussion

Our findings indicate that warming-induced drought stress and mistletoe infestation were the main stressors explaining the growth decline of the studied Scots pine populations in xeric sites. Our results suggest that if climate becomes drier, *P. sylvestris* will undergo significant growth reductions while those individuals infested by mistletoe may be not able to overcome this additional stress factor, likely inducing stand-level dieback. These results support taking into account biotic factors (mistletoes, fungi, and insects) in drought-prone forests as contributing drivers of warming-induced growth declines.

4.1. Effects of mistletoe infestation on intrinsic water use efficiency

In this study, severely infested trees grew less and recently they showed smaller increase in iWUE (+0.05 μmol mol^{-1} yr^{-1}) as compared with non-infested trees (+1.78 μmol mol^{-1} yr^{-1}), based on carbon isotopic data. This implies that the rate of iWUE rise as atmospheric CO_2 concentrations increase was almost nil in infested trees. Carbon discrimination supports that, on average, non-infested trees have higher iWUE than infested trees (about 8.4 μmol mol^{-1} yr^{-1} higher for the 2005-2008 period) whereas the BAI difference between non-infested and infested trees was about 2.5 cm^2 $year^{-1}$. However, these recent divergences were only evident after a pronounced drought occurred in 2005. The studied Scots pine populations showed a fairly stable discrimination rate since the 1980s and thus a constant c_i/c_a scenario may be assumed for these trees. These findings concur with other studies indicating that gains in iWUE were the result of rising CO_2 concentrations (c_a) rather than any functional responses by trees (Körner et al., 2007 and references therein). In the last analysed interval (2005-2008), the non-infested trees did decrease c_i/c_a as compared to the previous time period and such decrease was linked to the aforementioned deceleration of the iWUE increase of infested trees. The lack of growth and iWUE responses to the increase in carbon availability observed in infested trees agrees with other research confirming that rising CO_2 levels are not stimulating tree growth in drought-prone areas (Peñuelas et al., 2010). On the other hand, increasing water-use efficiency from a variety of tree species, exposed to

variable environmental conditions over time, seem to show species-specific ecophysiological mechanisms (Battipaglia et al., 2013). For instance, some tree species displayed downward adjustment of photosynthesis under elevated air CO_2 concentration (i.e. higher discrimination under elevated CO_2) in dry and nutrient-poor environments (Saurer et al., 2003).

Severely infested and non-infested trees showed similar values of carbon isotopic discrimination (between -24 and -25 ‰) along the ca. one half century studied here, although they were slightly lower in the infested trees for the last twenty years and significantly lower for the last five years. As a consequence, excluding the most recent period, long-term iWUE increases in a similar way for both infested and non-infested trees, while contrasting growth trends in response to drought and mistletoe abundance were significantly present as long as a decade prior to sampling. It has been hypothesized that rising atmospheric CO_2 concentrations could compensate for drought effects since increasing CO_2 partial pressure should allow to maintain tree carbon gain at a lower cost of water loss. If physiological or morphological tree adjustments allow photosynthesis rates (*A*; i.e. the carbon gain-related term in the iWUE) to be maintained, while stomatal conductance (*g*; the tree water status-related term in the iWUE) is reduced, then the iWUE should increases (Körner 2003). However, if drought-induced stomatal closure surpasses the CO_2-induced rising photosynthetic rate, carbon gain will decrease and therefore growth would decline. Our findings suggest that rising atmospheric CO_2 concentrations do not stimulate growth of infested trees under water-limited conditions, since the drought-induced reduction in photosynthesis rates and the warming-enhanced respiration costs override any positive effect caused by the increasing availability of atmospheric CO_2. In addition, we also illustrate how mistletoe infestation might be increasing the likelihood of warming- or drought-induced mortality on host trees, as the hemiparasite is constraining both the growth dynamics and the inferred water use of infested trees.

4.2. Effects of mistletoe infestation on tree growth and sensitivity to climate

Severely infested Scots pine trees showed a reduced basal area increment, as compared with the non-infested trees, after the 1994 and 2005 droughts. Such irreversible growth loss was not fully explained by drought stress alone, since non-infested trees did not present an equivalent growth decline. In *Pinus nigra* mistletoe seems to reach maximum infestation levels about 10 to 15 years after the colonization of the host tree started (Vallauri, 1998). This suggests that severely infested trees would show a decline in growth once a threshold of mistletoe abundance is surpassed. Indeed, in *Abies alba* Noetzli et al. (2004) detected that growth continuously declined in infested host trees once the mistletoe population

395 invaded the whole crown and occupied the main stem and branches. In the study area winter
396 temperatures steadily and significantly (P = 0.04) rose by ca. +0.01º yr^{-1} during the 20th
397 century. Such winter warming and the observed expansion of thrushes (Vorisek et al., 2008)
398 may have boosted mistletoe abundance in some Spanish pine stands (López-Sáez, 1993)
399 perhaps surpassing the mentioned threshold of mistletoe infestation.
400 The recent reduction in basal area increment caused by mistletoe was noticeable in all
401 sites (Fig. 2). This growth loss was also contingent on local conditions, since precipitation
402 variables were more relevant drivers of growth in the drier and less productive sites (e.g., site
403 PB). Mistletoes derive substantial amounts of water and carbon from their host trees and show
404 higher transpirations rates than the host trees (Marshall et al., 1994). Trees reduce its
405 transpiration rates through stomatal closure in response to drought but mistletoe continues
406 transpiring, thus increasing the water loss and drought stress experienced by host trees
407 (Fischer, 1983; Zweifel et al., 2012). It is therefore plausible that mistletoe infestation shifts
408 the biomass allocation pattern of host trees, changing for instance their leaf to sapwood ratio
409 (Sala et al., 2001), and increasing warming-induced drought stress in infested trees (Rigling et
410 al., 2010). On the other hand, infested trees might allocate more carbon to fine root production
411 to meet the extra water demand but this has not been tested to our knowledge.
412 Basal area increment in the infested trees responded more strongly to climate than in
413 non-infested trees during the analysed period (1954-2008). Such findings agree with those
414 found by Stanton (2007) in ponderosa pines infested by western dwarf mistletoe. Probably,
415 infested trees displayed a higher growth rate and hydraulic conductivity than non-infested
416 trees under wet conditions such as the early 1970s in our study case. Further, mistletoe
417 infestation induces a decline in apical growth (Zuber, 2004) which could lead to altered
418 biomass allocation favouring radial growth. Nevertheless, testing this last idea would require
419 a long-term monitoring of mistletoe infestation and defoliation in selected trees and
420 comparing dry *vs*. wet years to disentangle the mistletoe effects on growth and water use from
421 those due to ontogenetic changes in tree size.
422
423 *4.3. Characteristics and responses of infested trees to the combined effects of drought and*
424 *mistletoe*
425 We found that infested trees tend to have thicker diameters and more recent crown
426 defoliation and to show higher radial-growth rates in the past compared to non-infested trees.
427 The greater diameters of infested trees suggest that they are able to form more stem wood, and
428 probably display higher conductivity rates than non-infested trees. However, the bigger size

429 and growth rates of infested trees are not explained by differences in age or competition
430 degree as compared to non-infested trees. Therefore, in our case the oldest trees did not
431 present the highest infestation levels which might be the case if they have had more time to
432 accumulate mistletoes. Finally, tree height did not differ among infestation classes indicating
433 that infested trees were not necessarily those preferred by birds for perching and dispersing
434 mistletoe seeds.

435 Consistent with the negative impacts of drought and mistletoe on growth and iWUE of
436 Scots pine, Sala et al. (2001) and Meinzer et al. (2004) observed a decline in foliar $\delta^{13}C$
437 values of infested trees suggesting either a poor stomatal adjustment or a diminished
438 photosynthetic capacity in the host tree. Meinzer et al. (2004) found that photosynthesis rates
439 and needle nitrogen contents declined in infested trees. In Scots pine mistletoe-induced
440 stomatal closure allows avoiding hydraulic failure under short-term dry conditions but
441 severely reduces carbon uptake in the long term (Zweifel et al., 2012). These ecophysiological
442 findings suggest that trees show transient responses to different mistletoe infestation stages.
443 According to Galiano et al. (2011) mistletoe infestation would reduce growth by limiting
444 carbon assimilation, mediated by foliage loss and sapwood reduction. In summary, altered
445 growth patterns in severely infested trees are related to increased needle loss and decreasing
446 basal area increment. Overall, this indicates that severe mistletoe infestation alters the long-
447 term carbon source-sink balance.

448 Our findings suggest that the size and growth rates of host trees modulate how
449 mistletoe infestation affects tree performance. In agreement with this suggestion, dominant
450 trees were the most severely infested by mistletoe in Pyrenean silver fir forests (Oliva and
451 Colinas, 2007). Such results and the fact that this hemiparasite further decreases growth and
452 water-use efficiency in trees already stressed by drought indicate that we need a better
453 understanding of the interactions between host trees, mistletoes and climate warming to
454 forecast the future of pine stands affected by mistletoes in xeric sites (Dobbertin, 2005). Our
455 findings confirm that mistletoe infestation contributes to drought-induced forest decline in
456 xeric sites and mainly affects those trees showing the highest growth rates before infestation
457 proceeds. It may be worthy to evaluate if this pattern is general in other forests and
458 considering decline episodes induced synergistically by drought and other organisms (fungi,
459 insects).

460 In conclusion, mistletoe infestation and drought caused short-term growth and water-
461 use efficiency declines, leading to a reduced growth and sapwood production and enhancing
462 defoliation in Scots pine stands located near the southernmost limit of the species distribution.

463 Currently infested trees showed in the past higher growth rates than non-infested trees.
464 Infested trees had a higher growth responsiveness to water availability as compared to non-
465 infested trees, but in the last years the former did not improve their intrinsic water-use
466 efficiency as much as the later did. The cumulative effects of mistletoe and drought reduced
467 the intrinsic water-use efficiency in severely infested Scots pine trees by 9%, but this was
468 observed when host trees were severely infested. Mistletoe infestation and drought stress
469 reduced much more secondary growth than water-use efficiency.
470
471 *4.4. Management implications*
472 Mistletoes are keystone species for maintaining biodiversity since their fruits constitute one of
473 the main food resources for birds during the winter (Mathiasen et al., 2008). Birds feed on
474 mistletoe fruits and promote the long-distance dispersal and germination of the sticky and
475 sugar-rich mistletoe berries. Consequently, to reduce mistletoe dispersal it may be helpful to
476 plant and promote other shrub and tree species producing berries in winter, which can feed
477 birds, reducing mistletoe fruit consumption and seed dispersal. This could help to reduce the
478 incidence of mistletoe on the biggest trees, which usually show the highest growth rates
479 before infestation started. These dominant individuals are usually considered the most
480 valuable trees for wood extraction but they can also be selected perching sites for some bird
481 species, acting as initial infestation foci (Dobbertin and Rigling, 2006; Mathiasen et al.,
482 2008).
483 It would be also advisable to remove the biggest and most vigorous mistletoe female
484 indidividuals, usually colonizing the upper third of the tree crown (Sangüesa-Barreda et al.,
485 2012), before they start producing seeds. In drought-prone areas mistletoe removal should be
486 more effective before or while severe droughts occur, in order to reduce the combined
487 negative effects of both stressores on needle retention, tree growth, and water use efficiency.
488 In addition, removing and pruning out big mistletoe female individuals or heavily infested
489 branches would further decrease the overall production of mistletoe fruits and seeds and their
490 dispersal within the host tree (mistletoe seeds tightly stick to any branch or shoot that they fall
491 on) thus reducing the number of new infestations at the lower levels of the canopy.
492 In the last term, heavily infested trees could be selectively thinned to keep them in a
493 low density and widely separated to limit dispersal among neighboring trees and to alleviate
494 drought stress by decreasing tree density and competition for soil water (Dobbertin, 2005).
495 Mistletoes are hemiparasites. Therefore, their negative effects on tree water use may be more
496 noticeable under conditions of severe water deficit and mostly affect already stressed trees in

497 drought-prone habitats. Consequently, an effective and long-term control program of
498 mistletoe infestation should select the potentially most sensitive trees and stands to mistletoe
499 infestation, and it would require the combined efforts of researchers, managers, owners, and
500 public agencies.
501
502 **Acknowledgments**
503 This study was supported by projects CGL2007-66066-C04-02/BOS, CGL2008-04847-C02-
504 01 and CGL2011-26654 (Spanish Ministries of Science and Economy). JJC acknowledges
505 funding by ARAID and collaborative efforts within the Globimed network
506 (www.globimed.net). We thank the ICO and the Spanish Meteorological Agency for
507 providing bird ringing and climate data, respectively. We thank J. Lichstein and two
508 anonymous reviewers for their constructive comments on a previous version of the
509 manuscript. We sincerely thank colleagues from the Forest Health Laboratory (Mora de
510 Rubielos, Gobierno de Aragón) for their help and comments.
511

References

Allen, C.D., Macalady, A.K., Chenchouni, H., et al., 2010. A global overview of drought and heat-induced tree mortality reveals emerging climate change risks for forests. Forest Ecology and Management 259, 660-684.

Arbuckle, J.L., 1995-2009. Amos 18.0 User's Guide. SPSS, Chicago.

Battipaglia, G., Saurer, M., Cherubini, P., Calfapietra, C., McCarthy, H.R., Norby, R.J., Cotrufo, M.F. 2013. Elevated CO_2 increases tree-level intrinsic water use efficiency: insights from carbon and oxygen isotope analyses in tree rings across three forest FACE sites. New Phytologist 197, 544–554.

Bickford, C.P., Kolb, T.E., Geils, B.W., 2005. Host physiological condition regulates parasitic plant performance: *Arceuthobium vaginatum* subsp. *cryptopodum* on *Pinus ponderosa*. Oecologia 146, 179-189

Biondi, F., Qaedan, F., 2008. A theory-driven approach to tree-ring standardization: Defining the biological trend from expected basal area increment. Tree-Ring Research 64, 81-96.

Burnham, K.P., Anderson, D.R., 2002. Model Selection and Multimodel Inference: A Practical Information-Theoretic Approach. Springer-Verlag, Heidelberg.

Dobbertin, M., 2005. Tree growth as indicator of tree vitality and of tree reaction to environmental stress: a review. European Journal of Forest Research, 124, 319-333.

Dobbertin, M., Hilker, N., Rebetez, M., Zimmermann, N.E., Wohlgemuth, T., Rigling, A., 2005. The upward shift in altitude of pine mistletoe (*Viscum album* ssp *austriacum*) in Switzerland –the result of climate warming? International Journal of Biometeorology 50, 40-47.

Dobbertin, M., Rigling, A., 2006. Pine mistletoe (*Viscum album* ssp. *austriacum*) contributes to Scots pine (*Pinus sylvestris*) mortality in the Rhone valley of Switzerland. Forest Pathology 36, 309-322.

Farquhar, G.D., Richards, R.A., 1984. Isotopic composition of plant carbon correlates with water-use efficiency of wheat genotypes. Australian Journal of Plant Physiology 11, 539-552.

Farquhar, G.D., O'Leary, H.M., Berry, J.A., 1982. On the relationship between carbon isotope discrimination and the intercellular carbon dioxide concentration in leaves. Australian Journal of Plant Physiology, 9, 121-137.

544 Ferrio, J.P., Florit, A., Vega, A., Serrano, L., Voltas, J., 2003. $\Delta^{13}C$ and tree-ring width
545 reflect different drought responses in *Quercus ilex* and *Pinus halepensis*. Oecologia
546 137, 512-518.
547 Fischer, J.T., 1983. Water relations of mistletoes and their hosts. In: Calder M,
548 Bernhard T (eds) The Biology of Mistletoesk. Academic Press, Sydney, pp 163-184
549 Fritts, H.C., 1976. Tree rings and Climate. Academic Press, New York.
550 Galiano, L., Martínez-Vilalta, J., Lloret, F., 2010. Drought-induced multifactor decline
551 of Scots Pine in the Pyrenees and potential vegetation change by the expansion of
552 co-occurring oak Species. Ecosystems 13, 978-991.
553 Galiano, L., Martínez-Vilalta, J., Lloret, F., 2011. Carbon reserves and canopy
554 defoliation determine the recovery of Scots pine 4 yr after a drought. New
555 Phytologist 190, 750-759.
556 Glatzel, G., Geils, B.W., 2009. Mistletoe ecophysiology: host–parasite interactions.
557 Botany 87, 10-15.
558 Grace, J.B., 2006. Structural Equation Modeling and Natural Systems. Cambridge
559 University Press, Cambridge.
560 Hawksworth, F.G., 1977. The 6-Class Dwarf Mistletoe Rating System. USDA Forest
561 Service, Rocky Mountain Forest and Range Experiment station, Fort Collins.
562 Holmes, R.L., 1983. Computer-assisted quality control in tree-ring dating and
563 measurement. Tree-Ring Bulletin 43, 68-78.
564 Holmes, R.L., 1994. Dendrochronology Program Library. Laboratory of Tree-Ring
565 Research, The University of Arizona, Tucson.
566 Jöreskog, K.G., 1993. Testing Structural Equation Models. In: Bollen K, Long JS (eds)
567 Testing Structural Equation Models. Sage, Newbury Park, pp 294–316.
568 Körner, C., 2003. Carbon limitation in trees. Journal of Ecology 91, 4-17.
569 Körner, C., Morgan, J., Norby, R., 2007. CO_2 fertilization: when, where, how much? In:
570 Canadell J, Pataki DE, Pitelka L (eds) Terrestrial Ecosystems in a Changing World.
571 Springer-Verlag, Berlin, pp 9-21.
572 Lee, S.Y., 2007. Structural Equation Modeling: A Bayesian Approach. Wiley,
573 Chichester.
574 Linares, J.C., Camarero, J.J., 2011. From pattern to process: linking intrinsic water-use
575 efficiency to drought-induced forest decline. Global Change Biology 18, 1000-1015.

López-Sáez, J.L., 1993. Contribución a la corología y ecología del muérdago (*Viscum album* L.) en el centro y norte de la Península Ibérica. Boletín de Sanidad Vegetal y Plagas 19, 551-558.

Manion, P.D., 1991. Tree Disease Concepts. Prentice-Hall, Upper Saddle River.

Mapas Provinciales de Suelos, 1970. Provincia de Teruel. Mapa Agronómico Nacional. Instituto Geográfico y Catastral, Madrid.

Marshall, J.D., Ehleringer, J.R., Schulze, E.D., Farquhar, G., 1994. Carbon isotope composition, gas exchange and heterotrophy in Australian mistletoes. Functional Ecology 8, 237-241.

Martinez-Vilalta, J., Piñol, J., 2002. Drought-induced mortality and hydraulic architecture in pine populations of the NE Iberian Peninsula. Forest Ecology and Management 161, 247-256.

Mathiasen, R.L., Nickrent, D.L., Shaw, D.C., Watson, D.M., 2008. Mistletoes: pathology, systematics, ecology, and management. Plant Disease 92, 988-1006

McCarroll, D., Loader, N.J., 2004. Stable isotopes in tree rings. Quaternary Science Reviews 23, 771-801.

Meinzer, F.C., Woodruff, D.R., Shaw, D.C., 2004. Integrated responses of hydraulic architecture, water and carbon relations of western hemlock to dwarf mistletoe infection. Plant, Cell and Environment 27, 937-946.

Noetzli, K.P., Müller, B., Sieber, T.N., 2004. Impact of population dynamics of white mistletoe (*Viscum album* ssp. *abietis*) on European silver fir (*Abies alba*). Annals of Forest Science 60, 773-779.

Oliva, J., Colinas, C., 2007. Decline of silver fir (*Abies alba* Mill.) stands in the Spanish Pyrenees: role of management, historic dynamics and pathogens. Forest Ecology and Management 252, 84-97.

Peñuelas, J., Canadell, J., Ogaya, R., 2010. Increased water-use efficiency during the 20th century did not translate into enhanced tree growth. Global Ecology and Biogeography 20, 597-608.

R Development Core Team, 2013. R: A language and environment for statistical computing. R Foundation for Statistical Computing, Vienna. URL http://www.R-project.org.

Rigling, A., Eilmann, B., Koechli, R., Dobbertin, M., 2010. Mistletoe-induced crown degradation in Scots pine in a xeric environment. Tree Physiology 30, 845-852.

609 Robertson, I., Leavitt, S.W., Loader, N.J., Buhay, B., 2008. Progress in isotope
610 dendroclimatology. Chemical Geology, 252, EX1-EX4.
611 Roden, J.S., Farquhar, G.D., 2012. A controlled test of the dual-isotope approach for the
612 interpretation of stable carbon and oxygen isotope ratio variation in tree rings. Tree
613 Physiology 32, 490-503.
614 Sala, A., Carey, E.V., Callaway, R.M., 2001. Dwarf mistletoe affects whole-tree water
615 relations of Douglas fir and western larch primarily through changes in leaf to
616 sapwood ratios. Oecologia 126, 42-52.
617 Sangüesa-Barreda, G., Linares, J.C., Camarero, J.J., 2012. Mistletoe effect on Scots
618 pine decline following drought events. Insights from within-trees spatial patterns in
619 radial growth and carbon balance. Tree Physiology 32, 585-598.
620 Saurer, M., Cherubini, P., Bonani, G., Siegwolf, R. 2003. Tracing carbon uptake from a
621 natural CO_2 spring into tree rings: an isotope approach. Tree Physiology 23, 997–
622 1004.
623 Saurer, M., Siegwolf, R., Schweingruber, F., 2004. Carbon isotope discrimination
624 indicates improving water-use efficiency of trees in northern Eurasia over the last
625 100 years. Global Change Biology 10, 2109-2120.
626 Schomaker, M.E., Zarnoch, S.J., Bechtold, W.A., Latelle, D.J., Burkman, W.G., Cox,
627 S.M., 2007. Crown-condition classification: a guide to data collection and analysis.
628 Gen. Tech. Rep. SRS-102. USDA-Forest Service, Asheville.
629 Seibt, U., Rajabi, A., Griffiths, H., Berry, J.A., 2008. Carbon isotopes and water use
630 efficiency: sense and sensitivity. Oecologia 155, 441-454.
631 Stanton, S., 2007. Effects of dwarf mistletoe on climate response of mature ponderosa
632 pine trees. Tree-Ring Research 63, 69-80.
633 Tsopelas, P., Angelopoulos, A., Economou, A., Soulioti, N., 2004. Mistletoe (*Viscum*
634 *album*) in the fir forest of Mount Parnis, Greece. Forest Ecology and Management
635 202, 59-65.
636 Vallauri, D., 1998. Dynamique parasitaire de *Viscum album* L. sur pin noir dans le
637 bassin du Saignon (préalpes françaises du sud). Annales des Sciences Forestières 55,
638 823-835.
639 Vorisek, P., Gregory, R.D., Van Strien, A.J., Gmelig Meyling, A., 2008. Population
640 trends of 48 common terrestrial bird species in Europe: results from the Pan-
641 European Common Bird Monitoring Scheme. Revista Catalana d'Ornitologia 24, 4-
642 14.

643 Willmott, C.J., Rowe, C.M., Mintz, Y., 1985. Climatology of the terrestrial seasonal
644 water cycle. International Journal of Climatology 5, 589-606.
645 Zuber, D., 2004. Biological flora of Central Europe: *Viscum album* L. Flora 199, 181-
646 203.
647 Zuur, A.F., Ieno, E.N., Walker, N., Saveliev, A.A., Smith, G.M., 2009. Mixed Effects
648 Models and Extensions in Ecology with R. Springer, New-York.
649 Zweifel, R., Bangerter, S., Rigling, A., Sterck, F.J., 2012. Pine and mistletoes: how to
650 live with a leak in the water flow and storage system? Journal of Experimental
651 Botany 63, 2565-2578.

Figure captions

Figure 1. Selected structural equation model describing the effects of mistletoe infestation degree on crown cover and basal area increment in Scots pine. Goodness of fit statistics appear in the upper left part. Positive and negative effects are indicated by solid and dashed lines, respectively. Arrow widths are proportional to the absolute value of standardized path coefficients (numbers located near arrows). Only significant (P<0.05) coefficients are displayed. The observed variances of dependent variables (R^2) explained by the model are also presented. Unexplained variance, i.e. error terms, of each observed variable is indicated by arrows located near response variables. In the upper left corner several goodness-of-fit indices are indicated: the chi-square (χ^2) and its associated probability (P); the Adjusted Goodness-of-Fit Index (AGFI); the Akaike Information Criterion (AIC), and the Root Mean Square Error of Approximation (RMSEA). In relative terms, models with low AIC and RMSEA statistics, and also showing values close to one of the AGFI index and high P values associated with low χ^2 values correspond to better fits than models with the reverse characteristics.

Figure 2. Observed (thin lines) and predicted (thick lines) trends in basal area increment (BAI) based on linear mixed-effects models for non-infested (class ID1, trees without mistletoe) and infested trees (moderately ─class ID2─ and severely infested trees ─class ID3) considering the four study sites (SA, SB, PA, PB). BAI values are annual means ± SE. The three vertical lines indicate the severe droughts in 1986, 1994 and 2005. The percentages in the upper left corner of each graph indicate the amount of variability in BAI explained by the models.

Figure 3. Trends in the carbon isotopic ratio $^{13}C/^{12}C$ ($\delta^{13}C$) (a), isotopic discrimination between the carbon of atmospheric CO_2 and plant carbon (b), and inferred intrinsic water use efficiency (iWUE) (c) in non-infested trees (class ID1, empty symbols) and trees severely infested by mistletoe (class ID3, filled symbols). The values (means ± SE) are for five trees for each infestation class and considering 5-year intervals excepting the last segment (2005-2008). The carbon isotopic ratio in atmospheric CO_2 ($\delta^{13}C_{atm}$) and the rising atmospheric CO_2 concentrations are also presented.

683 **Tables**

684

685 **Table 1.** Geographical, topographical and structural features of the four study sites.

686

687

Site (code)	Latitude (N)	Longitude (W)	Altitude (m)	Aspect	Slope (º)	Basal area (m^2 ha^{-1})	Stem density (No. ha^{-1})
Solano de la Vega-zona Alta (SA)	40º 23' 15''	0º 41' 38''	1580	SE	19	16.5	556
Solano de la Vega-zona Baja (SB)	40º 23' 13''	0º 42' 17''	1520	SE	13	16.0	633
Puerto de Gúdar-zona Alta (PA)	40º 21' 46''	0º 42' 41''	1660	SW	0	19.4	711
Puerto de Gúdar-zona Baja (PB)	40º 21' 37''	0º 42' 26''	1500	SE	0	13.8	778

688

689

690 **Table 2.** Characteristics of the trees sampled in the four study sites (frequencies and mean ± SE values). Trees used in the fitting of Structural
691 Equation Models (SEM) are indicated in the third column. Age was estimated by counting rings on cores taken at 1.3 m.

692

693

Site	No. sampled and cored trees	No. trees used in SEM	Dead trees (%)	Age (years)	Dbh (cm)	Height (m)	Crown diameter (m)	Crown height (m)	Frequency of trees based on their mistletoe infestation degree (%)		
									ID1	ID2	ID3
SA	50	30	10	66.69 ± 2. 23	25.55 ± 1. 28	9.88 ± 0.36	5.36 ± 0.19	7.45 ± 0.34	60	20	20
SB	57	37	3	47.65 ± 1.58	20.26 ± 0.70	8.02 ± 0.28	4.70 ± 0.17	5.91 ± 1.91	70	10	20
PA	64	38	7	49.53 ± 1.05	21.04 ± 0.54	8.92 ± 0.19	4.59 ± 0.15	4.59 ± 0.15	44	36	20
PB	70	53	10	59.22 ± 3.35	23.45 ± 1.09	8.69 ± 0.49	4.62 ± 0.23	4.62 ± 0.23	47	23	30

694

695

696

697

Table 3. Comparison of structural and growth (basal area increment, BAI) variables among Scots pine according to their infestation degree (ID1, trees without mistletoe; ID2, moderately infested trees; ID3, severely infested trees) for trees sampled within plots in the four study sites (SA, SB, PA, PB). Mean ± SE values are displayed and related statistics (*F* ratio). Different letters indicate significant ($P<0.05$) differences among infestation classes. The BAI was calculated for the period 1995-2008. Age was estimated by counting rings on cores taken at 1.3 m.

Variable	Infestation degree	SA	*F*	SB	*F*	PA	*F*	PB	*F*
Dbh (cm)	ID1	22.3 ± 0.8a	15.3***	19.9 ± 0.6a	13.2***	20.0 ± 0.6a	9.8***	22.5 ± 1.1a	10.0***
	ID2	29.0 ± 1.2b		22.1 ± 1.7a		21.5 ± 0.7b		25.8 ± 1.1b	
	ID3	29.5 ± 1.2b		27.2 ± 1.6b		24.6 ± 0.9b		28.0 ± 1.0b	
Age (years)	ID1	67.5 ± 2.8	0.3	48.2 ± 1.2	0.8	51.2 ± 4.6	0.8	58.5 ± 5.9	0.9
	ID2	70.6 ± 5.3		47.1 ± 2.7		48.0 ± 4.0		58.6 ± 9.1	
	ID3	67.6 ± 3.9		47.5 ± 1.3		49.8 ± 4.1		60.3 ± 3.6	
Tree height (m)	ID1	9.1 ± 0.3	0.8	8.4 ± 0.3	1.9	8.5 ± 0.3	0.1	8.3 ± 0.5	0.2
	ID2	9.5 ± 0.6		8.4 ± 0.6		8.6 ± 0.2		8.4 ± 0.8	
	ID3	9.8 ± 2.0		9.4 ± 0.3		8.8 ± 1.7		8.9 ± 0.5	
Crown height (m)	ID1	7.0 ± 0.3	0.6	6.3 ± 0.3	0.1	6.1 ± 0.3	0.5	6.0 ± 0.4	0.28
	ID2	7.1 ± 0.5		6.0 ± 0.8		6.0 ± 0.3		6.6 ± 0.8	
	ID3	7.2 ± 0.5		6.4 ± 0.4		5.7 ± 0.3		6.1 ± 0.4	
Crown diameter (m)	ID1	4.9 ± 0.2a	3.5*	4.7 ± 0.1a	7.0*	4.5 ± 0.3a	4.5*	4.6 ± 0.2a	5.5**
	ID2	5.3 ± 0.3b		5.1 ± 0.5ab		5.0 ± 0.2ab		5.2 ± 0.4ab	
	ID3	5.7 ± 0.2b		5.5 ± 0.5b		5.6 ± 0.4b		5.9 ± 0.3b	
Crown cover (%)	ID1	82.9 ± 4.4a	39.6***	84.8 ± 2.5a	33.4***	79.6 ± 5.4a	30.5***	87.0 ± 3.2a	25.4***
	ID2	39.4 ± 5.4b		60.6 ± 6.5b		61.7 ± 4.6b		72.0 ± 7.1a	
	ID3	29.2 ± 4.5b		41.7 ± 6.3b		30.8 ± 5.5c		39.0 ± 6.6b	
BAI (cm^2 $year^{-1}$)	ID1	3.0 ± 0.3a	3.9*	3.7 ± 0.3	0.3	2.7 ± 0.5a	11.0*	6.1 ± 0.7ab	3.4*
	ID2	2.4 ± 0.5ab		3.6 ± 0.8		1.6 ± 0.3b		7.8 ± 1.5a	
	ID3	1.6 ± 0.3b		3.5 ± 0.9		1.5 ± 0.3b		4.3 ± 0.7b	
Sapwood area (%)	ID1	67.0 ± 1.9a	16.4***	72.7 ± 1.5	0.8	80.2 ± 3.1a	4.9*	79.5 ± 2.0a	6.7**
	ID2	52.1 ± 4.3b		71.6 ± 5.3		72.4 ± 4.1ab		72.7 ± 5.2ab	
	ID3	51.5 ± 2.9b		68.3 ± 3.9		66.2 ± 3.3b		68.3 ± 2.7b	

Significance levels: *$P < 0.05$; ** $P < 0.01$; *** $P < 0.001$.

727 **Table 4.** Basal area increment (BAI) variance (%) of Scots pines explained by climate
728 variables and by previous-year BAI (BAI_{t-1}) according to linear mixed-effects models.
729 The models were fitted considering the four study sites (SA, SB, PA, PB) and
730 comparing non-infested (class ID1, trees without mistletoe) vs. infested trees
731 (moderately ─class ID2─ and severely infested trees ─class ID3). The last two lines
732 summarize the percentage of variance explained by: temperature (Var. Temp.) and
733 precipitation (Var. Prec.) variables. Positive (+) and negative (–) effects on BAI are
734 indicated for the following climatic variables: TSEp, previous September temperature;
735 TNOp, previous November temperature; TDEp, previous December temperature; TMR,
736 March temperature; TMY, May temperature; TJL, July temperature; PSEp, previous
737 September precipitation; PNOp, previous November precipitation; PFE, February
738 precipitation; PMY, May precipitation; PJN, June precipitation; PJL, July precipitation;
739 PAU, August precipitation.
740

	SA		SB		PA		PB	
Fixed factors (effect)	ID1	ID2+ID3	ID1	ID2+ID3	ID1	ID2+ID3	ID1	ID2+ID3
BAI_{t-1} (+)	12.18	10.34	11.51	13.04	36.39	37.26	16.40	17.04
TSEp (–)							15.09	15.09
TNOp (–)		5.19	6.04	7.43		8.36		
TDEp (+)	3.14	7.62	3.40	6.70		3.48		
TMR (–)	14.36	18.35	16.79	16.96	11.41	11.54		
TMY (–)					24.50	14.16		6.34
TJL (–)	27.41	21.47	25.44	24.12			28.94	31.06
PSEp (+)	2.70	1.39						
PNOp (+)					4.60	2.49	3.71	2.48
PFE (+)			1.49	1.29				
PMY (+)							5.00	4.23
PJN (+)							3.61	2.05
PJL (+)		1.08				1.89		1.80
PAU (+)	2.11	2.49	2.97	3.63		3.40		
Var. Temp (%)	44.91	52.63	51.67	55.21	35.91	37.54	44.03	52.49
Var. Prec. (%)	4.81	4.96	4.46	4.92	4.60	7.78	12.32	10.56

Figures

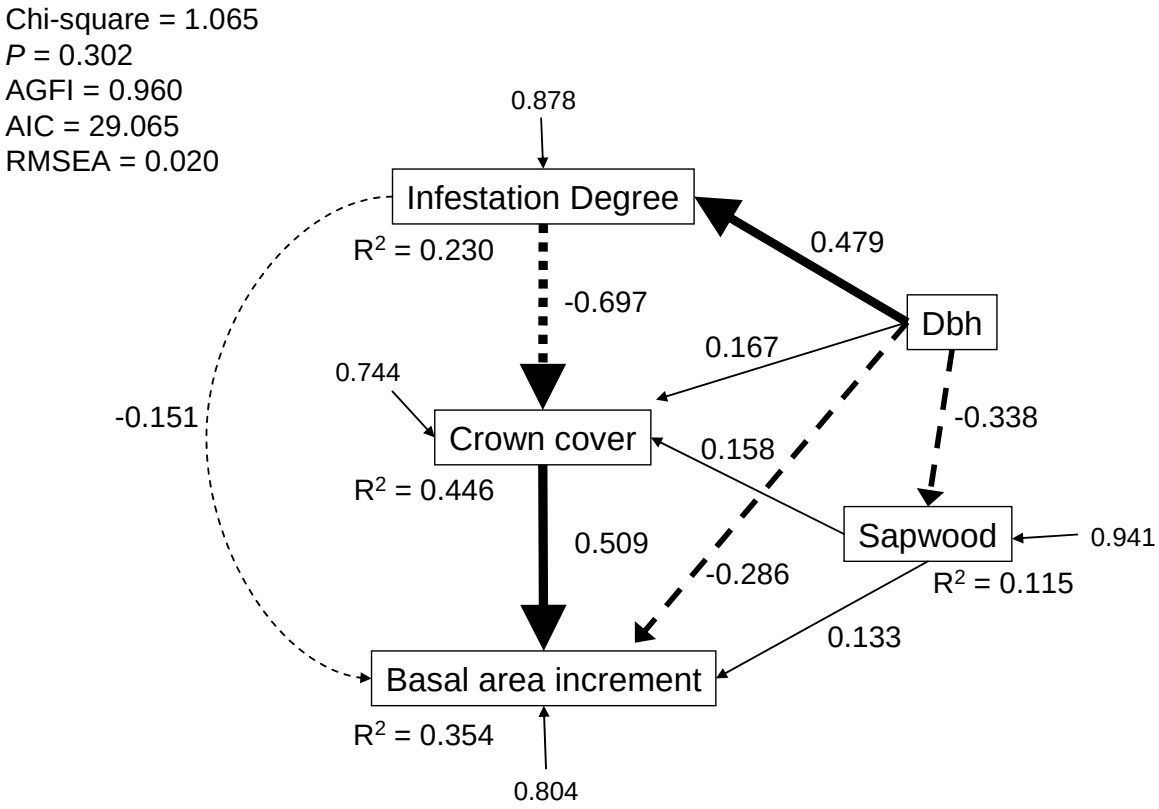

Figure 1

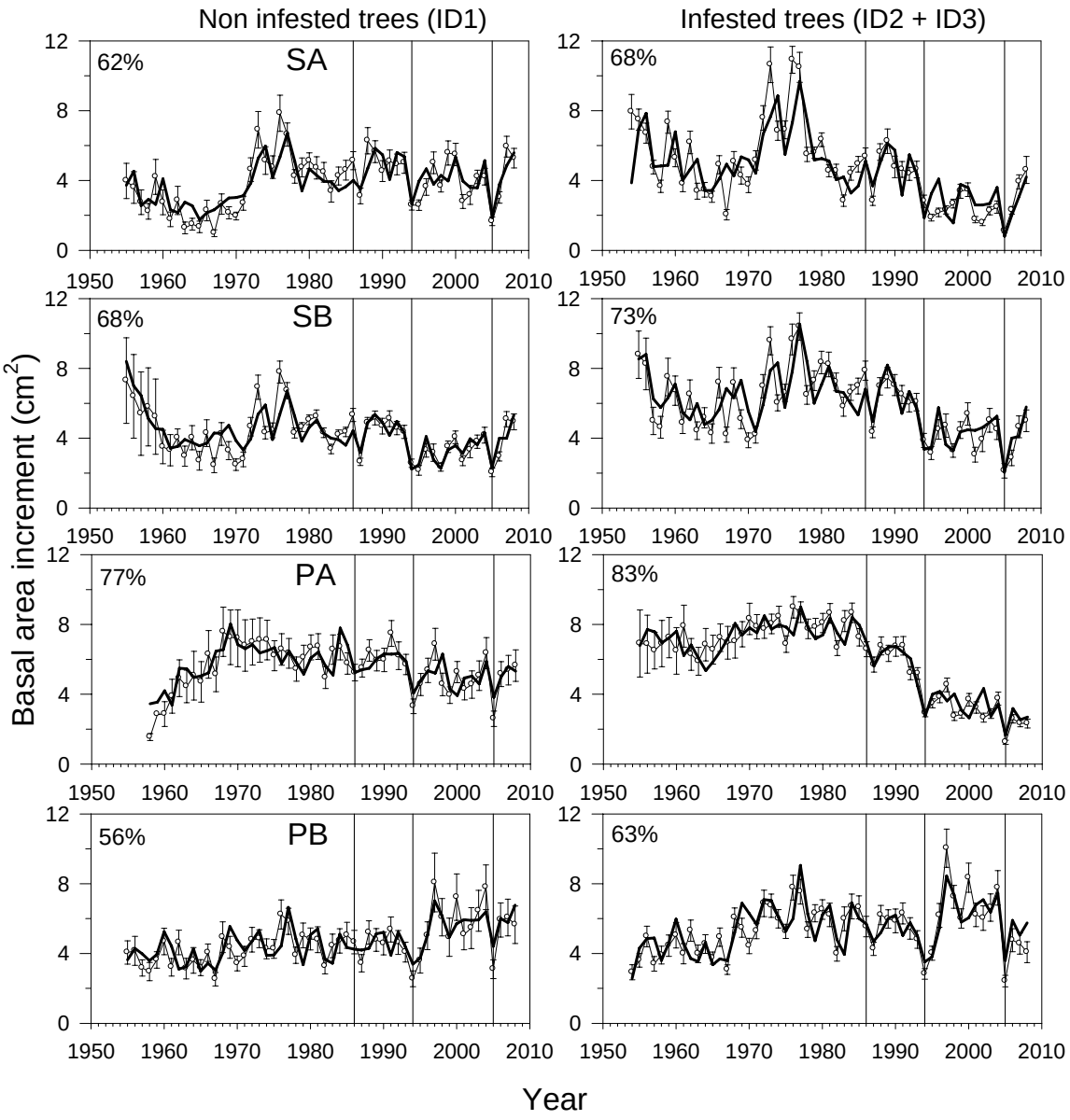
Non infested trees (ID1)
Infested trees (ID2 + ID3)
62%
SA
68%
68%
SB
73%
77%
PA
83%
56%
PB
63%
Basal area increment (cm2)
Year

Figure 2

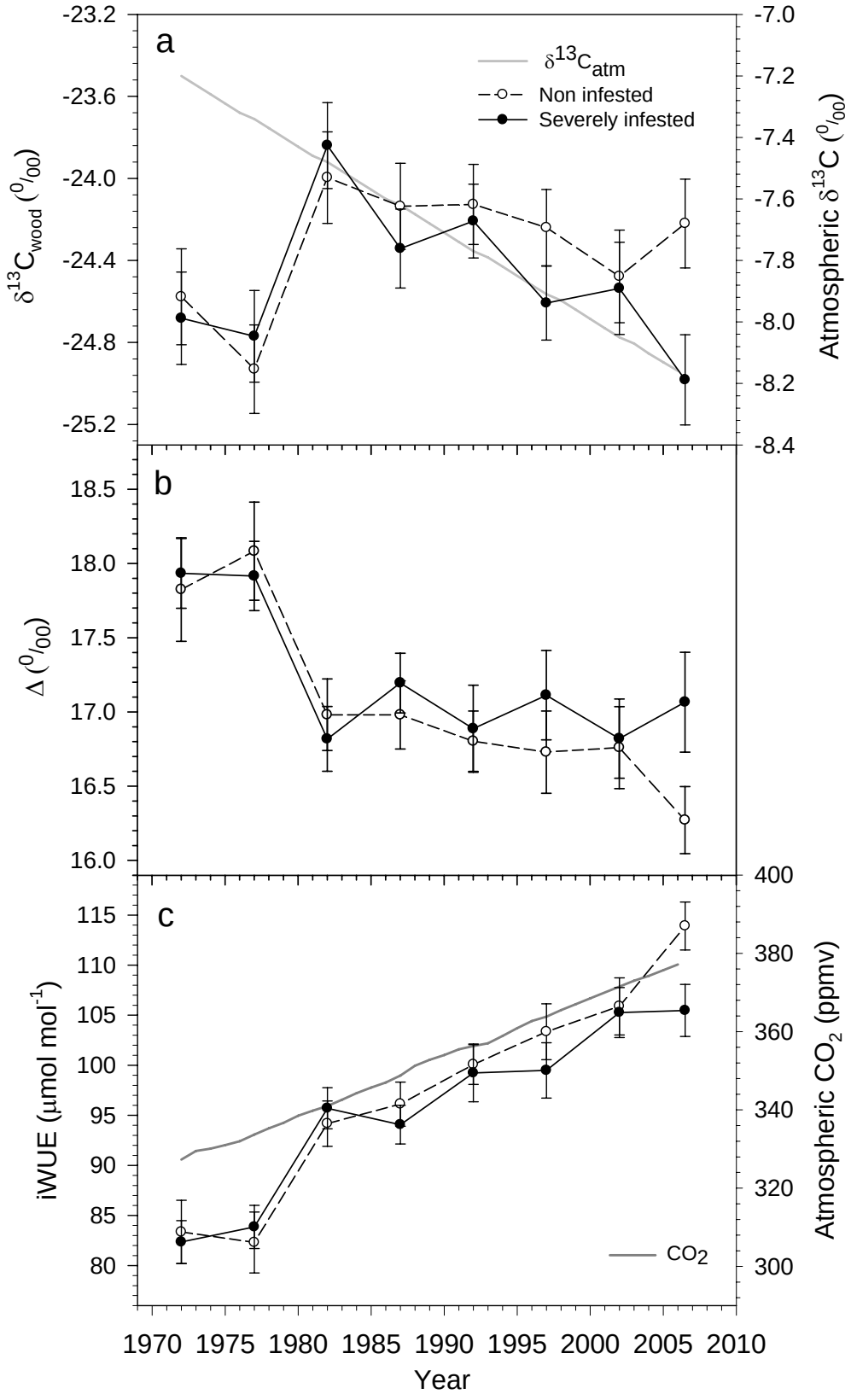
a
b
c
$\delta^{13}C_{atm}$
Non infested
Severely infested
$\delta^{13}C_{wood}$ (‰)
Atmospheric $\delta^{13}C$ (‰)
Δ (‰)
iWUE (µmol mol^{-1})
Atmospheric CO_2 (ppmv)
CO_2
-23.2
-23.6
-24.0
-24.4
-24.8
-25.2
-7.0
-7.2
-7.4
-7.6
-7.8
-8.0
-8.2
-8.4
18.5
18.0
17.5
17.0
16.5
16.0
115
110
105
100
95
90
85
80
400
380
360
340
320
300
1970 1975 1980 1985 1990 1995 2000 2005 2010
Year

Figure 3